Steady State and Time−Resolved Fluorescence Study of Residual Structures in an Unfolded Form of Yeast Phosphoglycerate Kinase †

ARTICLE *in* BIOCHEMISTRY · JUNE 1998

Impact Factor: 3.02 · DOI: 10.1021/bi973161x · Source: PubMed

6 AUTHORS, INCLUDING:

Fabienne Merola
Université Paris-Sud 11
58 PUBLICATIONS **882** CITATIONS

Steady State and Time-Resolved Fluorescence Study of Residual Structures in an Unfolded Form of Yeast Phosphoglycerate Kinase†

Pascal Garcia,‡,§ Fabienne Mérola,|| Véronique Receveur,‡,⊥ Patrick Blandin,|| Philippe Minard,‡ and Michel Desmadril*,‡

Laboratoire de Modélisation et d'Ingéniérie de Protéines, Bât. 430, Université Paris-Sud, 91405 Orsay Cedex, France, and Laboratoire pour l'Utilisation du Rayonnement Electromagnétique, Bât. 209D, Université Paris-Sud, 91405 Orsay Cedex, France

Received December 29, 1997; Revised Manuscript Received March 11, 1998

ABSTRACT: A previous study performed using steady state fluorescence has revealed the existence of residual structures surrounding the two tryptophan residues in an unfolded form of yeast phosphoglycerate kinase [Garcia, P., et al. (1995) *Biochemistry 34*, 397−404]. In this paper, we present a more detailed characterization of these residual structures, through the study of two single tryptophan-containing mutants of yPGK, W333F and W308Y. Denaturation experiments have first been performed at low temperatures to assess the nature of the interactions stabilizing these residual structures. On the other hand, the compactness and dynamics of the protein matrix were probed using tryptophan fluorescence quenching by acrylamide at various denaturant concentrations. Taking into consideration the changes in sample viscosity induced by addition of guanidinium chloride made feasible the use of this technique during the denaturation process. These different approaches have shown that the residual structures around tryptophan 308 are mainly stabilized by hydrophobic interactions and are more compact and less fluctuant than the ones surrounding tryptophan 333. Native and denatured yPGK have also been studied by time-resolved fluorescence spectroscopy. In the native protein, tryptophan buried in the core, W333, is mainly associated with a lifetime close to 0.1 ns, whereas tryptophan that is partially accessible to the solvent, W308, has a lifetime close to 0.5 ns. The time-resolved tryptophan fluorescence emission of wild-type yPGK can be accounted for quantitatively by the summed emissions of its two single tryptophan mutants. The significance of minor long lifetime components is discussed for the two tryptophan residues. This new assignment of fluorescent decay times has allowed for the detection of a folding intermediate in which the environment of tryptophan 333 is modified for denaturant concentrations lower than those for tryptophan 308.

The presence of residual structures in the denatured states of proteins has been widely studied during the ten last years. Different kinds of residual structures have been observed in the denatured states of hen egg white lysozyme (*1*), phage 434 repressor (*2*, *3*), ribonuclease A (*4*, *5*), bovine pancreatic trypsin inhibitor (*6*, *7*), FK506 binding protein (*8*), barnase (*9*), barstar (*10*), or the α-subunit of tryptophan synthase (*11*, *12*), and they may correspond to hydrophobic collapses, nonnative microstructures, or remaining elements of secondary structures. Recent reviews (*13*−*16*) have stressed the possible role of these residual structures in the folding process. They could act as initiation sites allowing the polypeptide chain to form the first elements of secondary structures through short-range interactions. Even though most of these studies have been carried out by using NMR spectroscopy, fluorescence spectroscopy has been useful in confirming the presence of residual structures in the denatured states of dihydrofolate reductase (*17*, *18*) and of a staphylococcal nuclease mutant (*19*). Previous folding studies of 3-phosphoglycerate kinase from yeast (yPGK)[1] have shown that the two tryptophan residues contained in this protein are involved in local residual structures (*20*).

The yPGK catalyzes the high-energy phosphoryl transfer of the acyl phosphate of 1,3-diphosphoglycerate to ADP to produce ATP. This monomeric protein with a molecular mass of 45 000 Da is folded in two globular domains. The tryptophan residues of the protein are located in the C-terminal domain, providing convenient probes for the studies of conformational changes of yPGK by fluorescence. The tryptophan in position 308 is quite accessible to the solvent, while the tryptophan in position 333 is completely buried in the center of the protein (*21*).

Two single tryptophan mutants have been constructed to study separately the spectroscopic properties of each tryp-

† This work was supported by the Centre National de la Recherche Scientifique and the Ministère de l'Enseignement Supérieur et de la Recherche.

* To whom all correspondence should be addressed.

‡ Laboratoire de Modélisation et d'Ingéniérie de Protéines.

§ Present address: Instituto de Estructura de la Materia, CSIC, Serrano 119, 28006 Madrid, Spain.

|| Laboratoire pour l'Utilisation du Rayonnement Electromagnétique.

⊥ Present address: New Chemistry Laboratory, OCMS, South Parks Road, Oxford OX1 3QT, U.K.

[1] Abbreviations: ADP, adenosine diphosphate; ATP, adenosine triphosphate; EDTA, ethylenediaminetetraacetate; Gdm-Cl, guanidinium hydrochloride; NATA, *N*-acetyltryptophanamide; yPGK, yeast phosphoglycerate kinase (EC 2.7.2.3); Tris, tris(hydroxymethyl)aminomethane.

S0006-2960(97)03161-9 CCC: $15.00
Published on Web 05/02/1998

tophan upon denaturation (*20*). To preserve the local environment of each tryptophan and minimize the steric constraints, tryptophans 308 and 333 were replaced by tyrosine (mutant W308Y) and phenylalanine (W333F), respectively. A previous study of the unfolding−refolding transition of these two mutants and the wild-type yPGK has shown that neither the catalytic activity nor the physicochemical properties of the enzyme were significantly altered by these mutations. The steady state fluorescence studies of the unfolding−refolding transition of the wild-type and mutant proteins have clearly revealed the existence of a hyperfluorescent intermediate (*20*, *22*). Indeed, the unfolding process induced by Gdm-Cl gives rise to two transitions, when it is followed by variation in fluorescence emission intensity at 350 nm. The first corresponds to an increase in fluorescence intensity, leading to a state of around 0.9 M Gdm-Cl with fluorescence higher than those of both the native and the fully denatured state. In this hyperfluorescent intermediate, while the activity and entire secondary structure have disappeared, the two tryptophans do not appear to be totally exposed to the solvent, as indicated by the position of maximum fluorescence emission. For higher Gdm-Cl concentrations, the second transition, accompanied by a decrease of fluorescence, corresponds to a further unfolding of the protein. This further unfolding has been attributed to the destruction of residual structures present in the hyperfluorescent intermediate as well as in the urea-denatured form of the enzyme (*20*). Another study of the unfolding transition of several yPGK mutants did not provide the evidence for the existence of this intermediate (*23*). This may be explained by the fact that these transitions have been followed up to only 2 M Gdm-Cl, which does not allow the observation of this form, as has been discussed before (*20*).

In this paper, we describe a further in-depth study of the nature of these residual structures. First, it has often been suggested that hydrophobic interactions are destabilized by low temperatures (*24*−*26*), and this suggestion has been used to probe the role of such interactions in stabilizing residual structures (*11*). Therefore, we have performed the study of the unfolding transitions of the two yPGK mutants at 6 °C which suggests a hydrophobic origin for the stabilization of the residual structures observed with the W333F mutant.

Second, information about the accessibility of the tryptophans during the denaturation process was obtained by acrylamide quenching studies. Although it provides important information about the dynamics and conformation of a protein, this technique has never been used to study the denaturation process. By using a model that takes into account the changes in viscosity due to the addition of denaturant, we could compare the compactness of the protein structure at various characteristic points of the transition curve.

On the other hand, using the intrinsic tryptophan fluorescence of yPGK as a probe of its denaturation process requires an understanding of its underlying composition. Contradictory data are found in the literature about the major components of the intrinsic fluorescence of yPGK. Early time-resolved fluorescence studies of the native wild-type yPGK have revealed that the tryptophanyl fluorescence decay can be resolved into two (*27*) or three (*28*) lifetime components. Another study of the fluorescence decay of the native wild-type yPGK has shown that both tryptophans have a heterogeneous emission with multiple decay lifetimes (*29*). These authors had attributed the shortest lifetime component (0.5 ns) to the buried tryptophan (in position 333) and the longer ones to the external tryptophan (in position 308). The buried tryptophan 333 would have a blue-shifted emission spectrum, totally inaccessible to all types of quencher, whereas the external tryptophan 308 emission can be separated into a blue-shifted emission, accessible to acrylamide and cesium only, and a red-shifted emission, accessible to acrylamide and iodide. However, all these tentative assignments are based on the a priori hypothesis that, according to the yPGK crystallographic structure, tryptophan 308 is more accessible to solvent than tryptophan 333.

A more recent study of yPGK at higher time resolution based on the survey of two single tryptophan mutants (*23*) revealed that each of the two fluorophores exhibits a minimum of three lifetime components with a short lifetime of 0.3−0.5 ns dominating in all cases the fluorescence decay. According to these authors, this short component would then represent a "marker" for both tryptophans in their native environment, whereas the two longer terms would correspond to the tryptophans in an "unfolded-like" environment.

Therefore, we have undertaken a careful time-resolved fluorescence study of the tryptophan of yPGK and its two single tryptophan mutants. Our results mainly confirm those of Szpikowska et al. (*23*) but, because of higher accuracy and statistics, reveal further details of the composition of each tryptophan emission. The fluorescence decay of the wild-type protein can now be quantitatively described by the sum of the decays of the two mutants. This allows in turn the assignment of specific lifetimes in the wild-type protein to each tryptophan in its native environment.

Time-resolved fluorescence was then used to investigate the denaturation process of wild-type and mutant yPGK as a function of Gdm-Cl concentration. The data collected demonstrate a sequential unfolding around W333 and W308 in the wild-type protein, with the latter residue retaining a native-like environment when W333 has already lost the interactions responsible for its efficient quenching.

MATERIALS AND METHODS

Wild-type yPGK and the W308Y and W333F mutants were prepared as described previously (*20*). All measurements were performed in 20 mM Tris-HCl buffer (pH 7.5) containing 0.5 mM EDTA and 1 mM 2-mercaptoethanol.

Steady State Fluorescence Studies of the Unfolding Transitions Induced by Gdm-Cl and Urea at 6 °C

Measurements were carried out with a 2 μM protein concentration after incubation for 12 h at 6 °C in different concentrations of Gdm-Cl or urea. To avoid the possible presence of cyanides (*30*), the urea was deionized on an Amberlite column and used within 1 day. Ultrapure urea and Gdm-Cl were obtained from Pierce. The denaturant concentrations were checked by refractometry, using the relationships provided by Nozaki (*31*) for Gdm-Cl and Warren and Gordon (*32*) for urea.

For each sample (i.e. each concentration of denaturant), a steady state fluorescence emission spectrum was recorded between 300 and 400 nm after excitation at 295 nm, with a

SLM 8000C Aminco spectrofluorometer and a 10 mm light path thermostated cell. To avoid the possible presence of condensation at 6 °C, the acquisition cell was maintained under a continuous nitrogen flow.

Transition curves were analyzed by a linear combination of two single transitions with opposite amplitudes, following the equation derived from the denaturant binding model, as described previously (*22*). To take into account the solvent effects on the signals corresponding to native and denatured proteins, the data were fitted to the following equation, by using a simplex procedure based on the Nelder and Mead algorithm (*33*).

$$y_x = y_N + S_N x + \left[\frac{\alpha_1 x^{n_1}}{C_{m_1}^{n_1} + x^{n_1}} + \frac{(1-\alpha_1)x^{n_2}}{C_{m_2}^{n_2} + x^{n_2}}\right][A + (S_D - S_N)x] \quad (1)$$

where y_N and y_D correspond to the fluorescence intensity of the native and denatured proteins, respectively, S_N and S_D are the solvent effects on the signal of the native and the denatured proteins, respectively, where C_{m_1} and C_{m_2} correspond to the transition midpoints of the first and the second transitions, respectively, n_1 and n_2 correspond to their cooperativity indexes, respectively, and α_1 corresponds to the relative amplitude of the first transition.

Studies of the Accessibility of the Tryptophan by Fluorescence Quenching Measurements

Measurements were carried out on the wild-type yPGK and the two mutants in the presence of 0, 2, and 4 M Gdm-Cl. Fluorescence quenching was also measured at Gdm-Cl concentrations corresponding to the hyperfluorescent form, i.e. 1, 0.7, and 0.9 M for wild-type yPGK, W308Y, and W333F mutants, respectively. So that the effects of viscosity changes on the diffusion of acrylamide were taken into account, fluorescence quenching of NATA by acrylamide was also measured in the presence of 0, 0.7, 0.9, 2, and 4 M Gdm-Cl. Proteins or NATA was incubated over the course of 12 h in the presence of those concentrations of Gdm-Cl, and then acrylamide at various concentrations was added. After further incubation for 2 h, a fluorescence emission spectrum was recorded as described above with a final protein concentration of 4 μM. The Gdm-Cl concentrations were checked by refractometry as in the unfolding transition experiments (see above). The final concentrations of acrylamide were checked by measuring the absorption at 295 nm (A_{295}), the reference being the 4 μM protein sample without acrylamide. A molar extinction coefficient of 0.23 M^{-1} cm^{-1} (*34*) was used for the conversion. The inner filter effect for light absorption by the acrylamide was corrected by using the correction factor proposed by Parker (*35*), $10^{A_{295}}$.

Stern−Volmer plots were constructed by using the variations of fluorescence intensity at 350 nm. The plots show an upward curvature, corresponding to an additional, static, quenching mechanism. To take into account both collisional and static quenching processes, the Stern−Volmer plots were fitted to the following equation (*36*):

$$\frac{F_0}{F} = (1 + K_{SV}[Q])e^{V[Q]} \quad (2)$$

where F_0 is the fluorescence intensity of the protein sample without acrylamide, F is the fluorescence intensity of the sample in the presence of a concentration [Q] of acrylamide, K_{SV} is the Stern−Volmer constant, and V is the static quenching constant. The Stern−Volmer constant K_{SV} is equal to $\tau_0 k_q$, where k_q is the bimolecular quenching constant and τ_0 is the fluorescence lifetime of the fluorophore in the absence of a quencher.

Time-Resolved Fluorescence Measurements

Sample Preparation. Protein samples and Gdm-Cl solutions were prepared as they were for steady state fluorescence studies. The denaturant concentrations were checked by refractometry as in the steady state fluorescence studies. The final concentration was 30 μM.

Measurements of Decays. Fluorescence decays were measured by the single photoelectron counting method (*37*). The experimental setup was installed on the SA1 beam line of the synchrotron radiation machine Super ACO at Laboratoire pour l'Utilisation du Rayonnement Electromagnétique (LURE, Orsay, France). Total fluorescence decays and fluorescence anisotropy decays were recorded as described in detail previously (*38*). The excitation was set at 300 nm ($\Delta\lambda = 6$ nm), and the emission was observed at 350 nm ($\Delta\lambda = 6$ nm). During the denaturation studies, the emission monochromator was set at zero order, and a high-pass cutoff filter at a wavelength ≥324 nm was used.

The instrumental function, $g(t)$, was recorded at the emission wavelength with a scattering solution of Ludox, alternately with the parallel and the perpendicular components of the fluorescence [$I_{VV}(t)$ and $I_{VH}(t)$, respectively]. The correction factor, β, for the differing sensitivities to polarization was determined as previously described (*38*). For each sample, approximately 10−20 millions counts were stored in the total fluorescence decay [$I_{VV}(t) + 2\beta I_{VH}(t)$] with each polarized curve being collected over 2048 channels at 23 ps/channel.

The level of scattered light present in our experiments was checked by using a nonfluorescent solution of Ludox adjusted to a scattering intensity similar to that of the sample. This level was determined to be less than $^1/_{1000}$ of the fluorescence signal.

Time-Resolved Fluorescence Analysis. An optimization procedure was performed as described by Blandin et al. (*38*) to minimize errors due to the variable time offsets between fluorescence and instrumental response. As pointed out previously (*38*, *39*), this time shift optimization is critical for a stable recovery of the shortest lifetimes present in some yPGK samples, and the results correlate well with changes in optical settings. This procedure allows a satisfactory description of the data starting at 1/100 of the leading edge of the decays.

Analysis of the fluorescence decays was performed by using the maximum entropy method, with the FAME program and MEMSYS2 as library subroutines (MEDC, Ltd.). After excitation by a vertically polarized pulse of light, and according to the complete expressions of the parallel [$I_{VV}(t)$] and the perpendicular [$\beta I_{VH}(t)$] components of the experimental fluorescence decay (*40*), the total intensity decay is obtained from the polarized component by the equation

$$F(t) = I_{VV}(t) + 2\beta I_{VH}(t) = g(t) \otimes \int_0^\infty \alpha(\tau) e^{-t/\tau}\, \partial\tau \quad (3)$$

where $g(t)$ is the measured instrumental function, $\otimes$ denotes a convolution product, and $\alpha(\tau)$, the preexponential factor distribution, represents the number of fluorophores with a fluorescence lifetime τ, assuming that all chromophores have identical radiative lifetimes and absorption coefficients at the excitation wavelength. According to this description, the analysis was then performed as described in detail previously (*38)*, except that 120 iterations were systematically performed.

The first-order average fluorescence lifetime $\langle\tau\rangle$ is then obtained from the lifetime distribution $\alpha(\tau)$ according to

$$\langle\tau\rangle = \frac{\int_0^\infty \tau\alpha(\tau)\, \partial\tau}{\int_0^\infty \alpha(\tau)\, \partial\tau} \quad (4)$$

The lifetime distribution $\alpha(\tau)$ is split in as many species as peaks separated by two well-defined minima. The lifetime τ_i and relative amplitude A_i of each species i are then defined by

$$\tau_i = \frac{\int_{\text{peak } i} \tau\alpha(\tau)\, \partial\tau}{\int_{\text{peak } i} \alpha(\tau)\, \partial\tau} \quad (5)$$

and

$$A_i = \frac{\int_{\text{peak } i} \alpha(\tau)\, \partial\tau}{\int_0^\infty \alpha(\tau)\, \partial\tau} \quad (6)$$

Error bars on individual lifetimes τ_i are based on the average width of the corresponding peak in the lifetime distribution. Error bars on average lifetimes $\langle\tau\rangle$ are based on estimates of the repeatability of the measurements.

RESULTS

It has been shown that the denaturation of yPGK and its single tryptophan mutants, when induced by Gdm-Cl at 20 °C, leads to an intermediate containing residual structures for denaturant concentrations around 1 M (*20*). Further addition of this denaturant leads to the destruction of these residual structures. To obtain further information about the nature of the transition, the equilibrium denaturation of mutants W308Y and W333F has been performed at 6 °C.

Equilibrium Denaturation at 6 °C

Mutant W333F. The transition curves obtained are monophasic (Figure 1), showing that at low temperatures the denaturation of this mutant corresponds to an apparent two-state process, different than the one observed at 20 °C. In a previous study (*20*), we showed that these residual structures were also present in the urea-unfolded protein, although the ones observed around the tryptophan in position 333 (mutant W308Y) seem less stable. The survey of the urea-induced denaturation of mutant W333F at low temperatures shows that the transition curve is also monophasic and presents the same amplitude as the Gdm-Cl-induced transition curve. The slope of the linear dependency of the fluorescence of a tryptophan observed when adding Gdm-Cl or urea is related to the degree of exposure of this fluorophore to the solvent. The slope of this dependency for the denatured mutant at 6 °C, expressed in percentage of NATA fluorescence in the absence of denaturant, has been compared to the dependency observed for a fully accessible tryptophan, the NATA molecule. The slopes corresponding to the tryptophan in the denatured mutant, whatever the denaturant used, are identical within experimental error to the ones observed for NATA: 3.0 ± 0.4 and 4.1 ± 0.4 in Gdm-Cl for the mutant and NATA, respectively, and 8.0 ± 0.6 and 9.1 ± 0.6 in urea for the mutant and NATA, respectively. Contrary to what happens at 20 °C, the denaturation of the mutant W333F at 6 °C seems to lead to a fully denatured state, in which the tryptophan would be totally accessible to the solvent, through a two-state model, which does not include an equilibrium intermediate possessing residual structures.

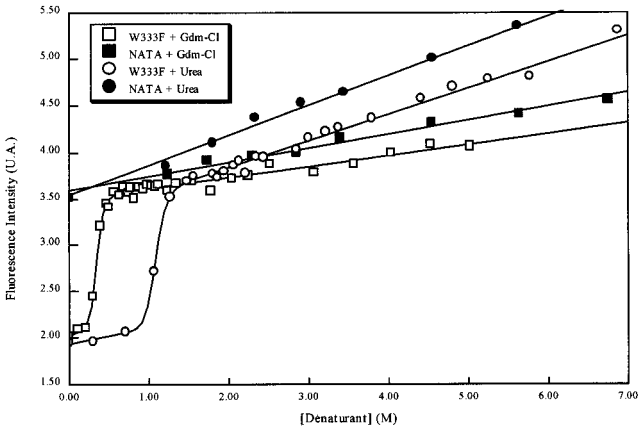

FIGURE 1: Denaturation transition curve at 6 °C of mutant W333F induced by Gdm-Cl and urea as assessed by the variation of the fluorescence intensity at 350 nm. These curves are superimposed with the curves corresponding to the variation of NATA fluorescence at 350 nm with denaturant concentration.

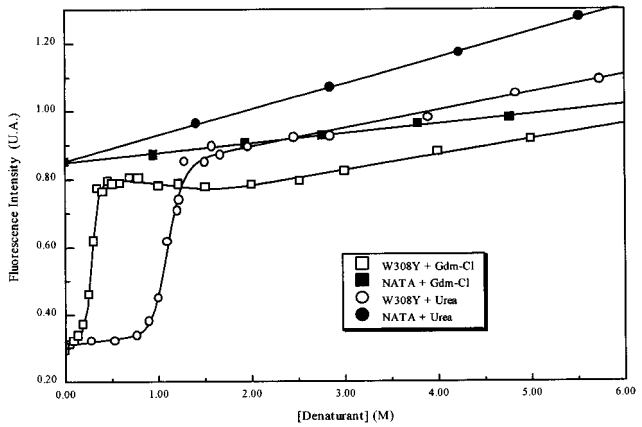

FIGURE 2: Denaturation transition curve at 6 °C of mutant W308Y induced by Gdm-Cl and urea as assessed by the variation of the fluorescence intensity at 350 nm. These curves are superimposed with the curves corresponding to the variation of NATA fluorescence at 350 nm with denaturant concentration.

Mutant W308Y. The transition curve corresponding to the denaturation of this mutant by Gdm-Cl at 6 °C remains biphasic, like the one observed at 20 °C (Figure 2). However, the midpoint of the first transition observed at 20 °C is shifted toward a lower concentration of denaturant

when the denaturation is performed at 6 °C, whereas the second transition midpoint is close to that observed at 20 °C. Since this second transition is still present in the denaturation at 6 °C (although with a lower amplitude), this would mean that the role of hydrophobic interactions in the stabilization of the residual structures around tryptophan 333 is less important than in the case of tryptophan 308.

Accessibility of the Two Tryptophans to Acrylamide by Fluorescence Quenching

Studying the quenching of protein's intrinsic fluorescence affords information about their conformation and dynamics. Although this technique has been used to study numerous proteins during the past twenty years (*41*), the denaturation process has almost never been investigated by fluorescence quenching. It is mainly due to the difficulty of keeping constant all parameters that could interfere with fluorescence properties, while the denaturation process is generally induced by varying factors inducing changes in fluorescence properties. Nevertheless, a study of lactate deshydrogenase denaturation induced by Gdm-Cl has allowed the determination of quenching constants, by taking into account the changes in viscosity (*42*).

In this work, wild-type yPGK and the two single tryptophan mutants have been studied in four different Gdm-Cl concentrations. The native proteins and the denatured ones have been investigated, as well as the so-called "hyperfluorescent" forms. The denatured states were studied in the presence of 2 and 4 M Gdm-Cl. To take into account the changes in viscosity induced by the variation of denaturant concentration, the model of "penetration" was used (*34*). This model involves a two-step diffusional process and affords conformational information from the Stern−Volmer plots. This mechanism describes a diffusion of the quencher molecule toward the surface of the protein, followed by a migration of this molecule toward the fluorophore, through the protein matrix of which the conformation is unknown. It can be represented by the following scheme:

$$\mathrm{Q} + \mathrm{P\text{-}Trp^*} \underset{k_{-d}}{\overset{k_d}{\rightleftharpoons}} (\mathrm{Q}\cdots\mathrm{P\text{-}Trp^*}) \xrightarrow{\chi} (\mathrm{P\text{-}Trp^*}\cdot\mathrm{Q}) \xrightarrow{k_i} \text{quenching}$$

where the external diffusion step (k_d and k_{-d}) is under viscosity control, whereas the internal migration step through the proteic matrix (χ) depends on the protein conformation only. Since the quenching step k_i is sufficiently rapid in comparison to the two previous steps, the apparent quenching constant, $k_{q(app)}$, is given by

$$k_{q(app)} = \frac{\chi k_d}{\chi + k_{-d}} \tag{7}$$

Since there is no affinity between the protein and the quenching molecule, the first equilibrium constant in the penetration model may be considered equal to 1, and thus, $k_d \approx k_{-d}$. The previous equation can therefore be written as

$$k_{q(app)} = \frac{\chi k_d}{\chi + k_d} = \frac{K_{SV}}{\tau_0} \tag{8}$$

The apparent quenching constant, given by the Stern−Volmer plots, is therefore split into two parts: a diffusion constant, k_d, only depending on the viscosity, and a penetration constant, χ, only depending on the protein conformation. The apparent quenching constant can thus give us the penetration constant provided we know the diffusion constant.

Thus, a fluorescence quenching study affords us two different kinds of information. (i) The static quenching constant, *V*, gives us the probability of finding a quencher molecule in contact with the fluorophore at the excitation time, this probability being inversely proportional to the steric shielding of the studied tryptophan by the protein matrix. (ii) The penetration constant, χ, gives us information about the rate of quencher penetration through the protein core, this rate being linked to the protein dynamics.

Variation of the Diffusion Constant with the Viscosity of the Solvent

For a fully accessible fluorophore, such as NATA, $\chi \gg k_d$, and thus $k_{q(app)}$ may be considered equal to k_d. The diffusion constant of the acrylamide molecule has then been determined by studying the quenching of NATA fluorescence in the presence of various Gdm-Cl concentrations. The Stern−Volmer constants corresponding to the NATA fluorescence quenching in the presence of five concentrations of Gdm-Cl are presented in Table 1, with the corresponding bimolecular quenching constants, k_q, and the static quenching constants, *V*.

The static quenching constants obtained are close to 2 M^{-1}, which corresponds to the previously published values (*43*). This parameter does not vary much, which can be explained by the fact that it only represents the probability of finding an acrylamide molecule in a given volume around the fluorophore during the excitation time.

It has been shown previously that the behavior found for acrylamide quenching of NATA fluorescence shows a viscosity dependence typical of a diffusion-limited reaction (*34*). The bimolecular quenching constants determined on NATA have then been used as diffusion constants in eq 9.

Study of the Accessibility of Tryptophans 308 and 333 in Various Conformational States of yPGK Mutants

Substituting eq 8 into eq 2 gives

$$\frac{F_0}{F} = \left(1 + \tau_0 \frac{\chi k_d}{\chi + k_d}[\mathrm{Q}]\right) e^{V[\mathrm{Q}]} \tag{9}$$

The parameters χ and *V* are obtained by fitting eq 9 to the experimental data, by using the simplex procedure based on the Nelder and Mead algorithm (*33*). The fittings are shown in Figure 3 and the obtained parameters in Table 2.

In the two native mutants, the absence of static quenching indicates that the two tryptophans are protected from such a big molecule as acrylamide by the polypeptide chain (*44*). The value of χ obtained for the mutant W308Y is also very low, which is also consistent with the position of tryptophan 333, buried in the core of the protein. However, the χ value obtained for the W333F mutant is surprisingly high, when compared to the *V* value obtained for this mutant. This might be explained by the dynamics of the protein, which allows

Table 1: Stern−Volmer Constants (K_{SV}), Bimolecular Quenching Constants (k_q), and Static Quenching Constant (V) Corresponding to NATA in the Presence of Five Different Gdm-Cl Concentrations[a]

[Gdm-Cl] (M)	V (M^{-1})	K_{SV} (M^{-1})	$k_q/10^9$ (M^{-1} s^{-1})
0	2.02 ± 0.04	18.00 ± 0.71	6.00 ± 0.24
0.7	2.19 ± 0.12	17.58 ± 0.96	5.86 ± 0.32
0.9	2.11 ± 0.05	15.44 ± 1.32	5.15 ± 0.44
2	1.91 ± 0.05	14.59 ± 0.57	4.86 ± 0.19
4	2.35 ± 0.13	10.71 ± 1.42	3.57 ± 0.47

[a] The mean fluorescence lifetime of NATA in the presence of the Gdm-Cl concentrations has been determined experimentally and is equal to 3 ns.

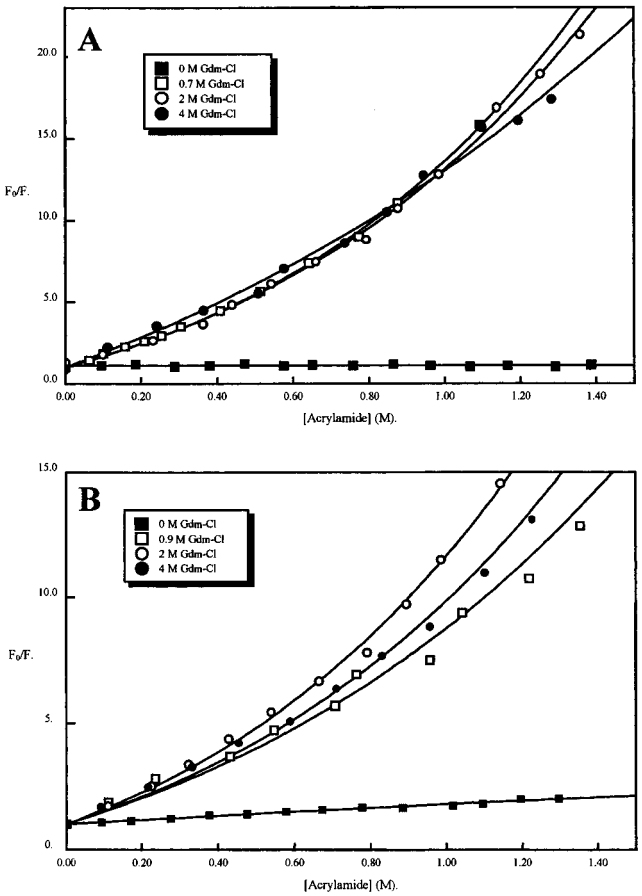

FIGURE 3: Stern−Volmer plots of the fluorescence quenching of mutant W308Y (A) and mutant W333F (B) in the presence of various Gdm-Cl concentrations. The fluorescence intensity is followed at 350 nm. The curves are fitted according to eq 9.

the quencher molecule to reach tryptophan 308 despite the steric shielding. Indeed, a study of the accessible area of the residues has shown that, using a normalized accessibility on a range from 0 to 1, tryptophans 308 and 333 would have accessible surfaces equal to 0.26 and 0, respectively (*21*). However, these values obtained from a static crystallographic structure may underestimate dynamic aspects, which could increase the penetration constant. Such a bias was shown for cystein accessibility in horse muscle PGK (*45*). In addition, since the two mutants have a lower stability than the wild-type form, they may also show a higher accessibility than the wild-type structure.

The study of the static quenching constant, V, reveals that during the unfolding process the tryptophans in yPGK become more accessible to acrylamide without, however, becoming as accessible as NATA. Indeed, the V value increases up to about 0.70 M^{-1}, while the value found during the study of NATA and in previous studies (*43*) is 2 M^{-1} for a fully accessible tryptophan. This indicates that the static quenching process is modified in a fully denatured protein by the steric shielding due to the unfolded polypeptide chain.

However, it may be noted that the V value obtained for the mutant W333F in the presence of 0.9 M Gdm-Cl (0.53 M^{-1}) is not as high as the ones obtained for fully denatured proteins. This would indicate that the residual structures surrounding tryptophan 333 in the hyperfluorescent intermediate are less compact than the ones that exist around tryptophan 308 in this state, which is consistent with the previously published results (*20*).

The χ values obtained for the Gdm-Cl concentrations corresponding to the hyperfluorescent intermediate clearly show that the dynamics of the proteins is different from the ones in the denatured forms. The residual structures present in the environment of the two tryptophans in these forms thus seem to modify significantly their dynamic accessibility to acrylamide. It also appears that the residual structures that exist around tryptophan 333 are more dynamic than the ones surrounding tryptophan 308.

Time-Resolved Fluorescence Study of yPGK

Time-Resolved Fluorescence of Wild-Type yPGK and Mutants in Their Native Forms. The lifetime distributions obtained for the three native proteins are shown in Figure 4A−C, and the parameters are presented in Tables 3 and 4. Up to five fluorescence decay times can be separated in the lifetime distributions of the wild-type yPGK. Two components at 0.1 ns (27%) and 0.5 ns (70%) strongly dominate the distribution, while several long lifetimes account for the remaining 3% of the pre-exponential amplitude. The lifetime distribution of W308Y shows evidence of four lifetimes similar to the ones observed in the wild type, but with a high weight (77%) of the very short term at 0.1 ns. Finally, W333F shows a somewhat less complex profile, dominated by 98% of a 0.5 ns component, and a very low contribution of two longer lifetimes.

These results, although more complex than all previously published, are in rather good agreement with what is currently known of yPGK tryptophan fluorescence (*23*, *27*−*29*), bringing the consistent picture, for the wild-type protein, of a decay dominated by a 0.4 ns term, characteristic of a strong dynamic quenching, but including also minor and multiple long lifetimes. We obtain a first-order average lifetime of 0.47 ns for wild-type yPGK, while the reported values range from 0.52 to 0.73 ns. For the mutants, our results are also in rough agreement with the data reported by Szpikowska et al. (*23*), for their mutants W333F and W308F, as can be estimated from the parameters shown in their Figure 6. However, our data clearly differ in the separation of a very short lifetime of 0.1 ns, never reported before, which actually appears as the dominant component of the W308Y emission in terms of relative population. Considering its very short duration, this fluorescence decay time must be carefully examined to distinguish it from a possible artifact.

First, because of its high contribution to the signal in W308Y, and according to the scatter tests we have performed

Table 2: Parameters Corresponding to the Quenching Process of yPGK Tryptophan Fluorescence Quenching in the Presence of Various Gdm-Cl Concentrations

mutant	[Gdm-Cl] (M)	$k_{d,\eta}{}^a/10^9$ (M^{-1} s^{-1})	$\langle\tau_0\rangle^b$ (ns)	V (M^{-1})	$K_{SV(app)}$ (M^{-1})	$k_{q(app)}/10^9$ (M^{-1} s^{-1})	$\chi/10^9$ (M^{-1} s^{-1})
	0	6.00	0.64	−	0.12 ± 0.10	0.19	0.10 ± 0.01
W308Y	0.7	5.86	2.15	0.72 ± 0.04	5.65 ± 0.15	2.62	4.76 ± 0.26
	2	4.86	2.19	0.66 ± 0.03	5.80 ± 0.31	2.65	5.82 ± 0.52
	4	3.57	2.22	0.71 ± 0.06	4.90 ± 0.35	2.21	5.81 ± 1.00
	0	6.00	0.56	−	0.96 ± 0.10	1.71	2.43 ± 0.20
W333F	0.9	5.15	1.98	0.53 ± 0.06	4.15 ± 0.42	2.10	3.53 ± 0.58
	2	4.86	1.86	0.69 ± 0.03	4.82 ± 0.27	2.59	5.54 ± 0.60
	4	3.57	1.89	0.64 ± 0.04	4.18 ± 0.29	2.21	5.82 ± 1.00

[a] Diffusion constant determined from NATA quenching studies. [b] Mean fluorescence lifetime determined from time-resolved fluorescence studies.

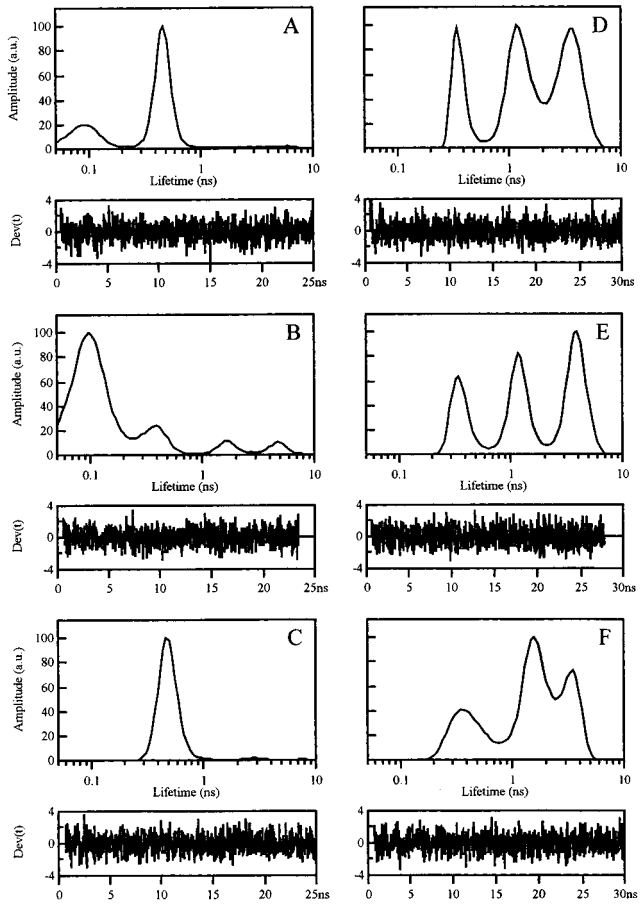

FIGURE 4: Tryptophan fluorescence lifetime distributions of wild-type and mutant yPGK in the absence (A−C) and presence (D−F) of 5 M Gdm-Cl: (A and D) wild-type yPGK, (B and E) mutant W308Y, and (C and F) mutant W333F.

(see Materials and Methods), it cannot simply be accounted for by contaminant scattered light. It is present with similar weights, whether the tryptophan emission is detected at 350 nm with a narrow band-pass or if all wavelengths are collected above 324 nm with a cutoff filter (see Table 4). This short component is also readily extracted whatever the method of analysis; the maximum entropy lifetime distributions give clear-cut evidence for a well-separated and stable entity. In standard nonlinear least-squares analysis, going from a three-exponential to a four-exponential model produces in all cases a strong improvement of the fit, with χ^2 decreasing from 3.1 to 1.2 in wild-type yPGK, from 2.8 to 1.2 in W308Y, and from 1.3 to 1.06 in W333F. Meanwhile, these least-squares analyses (Table 4) provide kinetic parameters in perfect agreement with the maximum entropy results (Table 5), with the exception of the W333F mutant, where the least-squares analysis results in a splitting of the major 0.5 ns component between two terms at 0.4 and 0.6 ns, for which the maximum entropy lifetime distribution does not give any evidence. It is unlikely, however, that the quality of our data would allow the separation of such close components, and we thus consider this solution an artifact inherent to the discrete exponential model used in the least-squares method (*46*, *47*).

A short 0.1 ns lifetime may be easily overlooked as soon as the information contained in the early time range of the data is lost experimentally or discarded during the analysis. There are many reasons why the information contained in this short time range can be missed, a major one being the absence of correction for variable time shifts (see Materials and Methods). In Table 4 are shown for illustration the results of nonlinear least-squares analyses performed on our data truncated in the short time range, showing that parameters very similar to those observed in the literature can be recovered under these conditions. In such partial analysis, because of the underestimation of the weight of the short components, the average lifetime is significantly increased, as is also the apparent relative weight of the long lifetime terms.

Assignment of Fluorescence Lifetimes in Wild-Type yPGK. We observe the 0.1 ns component systematically in the W308Y and in the wild-type form, while it is completely absent from the emission of W333F as well as in calibration experiments with NATA. The domination of this short lifetime in the emission kinetics of W308Y is in line with its reported strong quenching, resulting in a very low quantum yield of about 2% (*23*; unpublished results from our laboratory). Inclusion of this short component actually helps in understanding the time-resolved fluorescence of wild-type yPGK in terms of the relative contribution of each of these two residues. The two major peaks in its lifetime distribution can now be identified by the respective contributions of its two tryptophan residues, the 0.1 ns peak being exclusively ascribed to tryptophan 333 while the 0.5 ns being predominantly due to tryptophan 308. As Szpikowska et al. (*23*) showed previously that the steady state emissions of the two residues in the mutants could generate spectra identical to those of the wild-type form, addition of the fluorescence decay parameters of W308Y and W333F leads to average values in good agreement with those observed for the wild-type enzyme (Table 3). The slightly higher weighting of the 0.5 ns component observed in the experimental decay may result from slightly unequal weighting of

Table 3: Tryptophan Fluorescence Decay Parameters for Wild-Type yPGK and Mutants W308Y and W333F, Obtained from Maximum Entropy Analysis

yPGK[a]	τ_1 (ns) ± 0.05	A_1 (%)	τ_2 (ns) ± 0.1	A_2 (%)	τ_3 (ns) ± 0.5	A_3 (%)	τ_4 (ns) ± 1	A_4 (%)	$\langle\tau\rangle$ (ns) ± 10%	χ^2
WT	0.10	26.5	0.47	70.1	2.2[b]	2.3[b]	5.3	1.1	0.47	1.09
W308Y (1)	0.11	77.1	0.43	13.6	1.7	5.0	4.9	4.2	0.43	1.10
W333F (2)	−	−	0.50	98.1	2.9	1.5	7.0	0.4	0.56	0.96
50% (1) + 50% (2)	0.11	39	0.49	56	2.0	3.2	5.1	2.3	0.49	−

[a] At 20 °C and pH 7.5, with excitation at 300 nm and emission detected at 350 nm. τ_i is the fluorescence lifetime, A_i the relative amplitude, and $\langle\tau\rangle$ the average fluorescence lifetime. [b] Average of two consecutive peaks.

Table 4: Tryptophan Fluorescence Decay Parameters for Wild-Type yPGK and Mutants W308Y and W333F, Obtained from Nonlinear Least-Squares Analysis

yPGK	τ_1 (ns)	A_1 (%)	τ_2 (ns)	A_2 (%)	τ_3 (ns)	A_3 (%)	τ_4 (ns)	A_4 (%)	$\langle\tau\rangle$ (ns)	χ^2
wild-type[a]	−	−	0.42	90.7	1.2	7.2	5.1	2.1	0.57	1.84
W308Y[a]	−	−	0.34	74.7	2.1	16.6	5.7	8.7	1.09	1.29
W333F[b]	−	−	0.48	95.2	1.5	3.9	5.7	0.9	0.57	1.30
wild-type[b]	0.12	29.8	0.49	66.5	2.0	2.3	5.4	1.4	0.48	1.19
W308Y[b]	0.11	78.5	0.49	13.1	2.3	5.5	5.8	2.9	0.45	1.21
W333F[b]	0.43	29.0	0.66	69.0	2.7	1.5	6.9	0.5	0.56	1.06

[a] Leading edge of the data truncated. [b] All data points fitted starting from H/100 of the leading edge.

Table 5: Tryptophan Fluorescence Decay Parameters for Wild-Type yPGK and Mutants W308Y and W333F in the Presence of Various Gdm-Cl Concentrations, Obtained from Maximum Entropy Analysis

yPGK[a]	[Gdm-Cl] (M)	τ_1 (ns) ± 0.05	A_1 (%)	τ_2 (ns) ± 0.1	A_2 (%)	τ_3 (ns) ± 0.5	A_3 (%)	τ_4 (ns) ± 1	A_4 (%)	$\langle\tau\rangle$ (ns) ± 10%	χ^2
	0	0.09	27.7	0.47	68.9	1.9	1.8	5.1	1.7	0.48	1.00
	0.7	−	−	0.43	78.1	1.8	14.5	4.6	7.0	0.97	1.05
wild-type	1	−	−	0.42	22.0	1.4	39.0	3.7	38.9	2.08	1.07
	2	−	−	0.47	24.1	1.5	40.4	3.7	35.5	2.04	1.06
	5	−	−	0.44	17.6	1.3	37.6	3.5	44.7	2.18	0.98
	0	0.14	76.0	0.63	10.6	2.1	7.9	5.4	5.4	0.64	0.95
	0.55	0.18	34.7	1.01		32.9		3.9	32.3	1.64	1.01
W308Y	0.7	−	−	0.36	23.3	1.2	33.5	3.9	43.0	2.15	0.98
	2	−	−	0.50	29.5	1.5	29.9	3.9	40.4	2.19	0.96
	5	−	−	0.42	26.8	1.4	29.6	3.9	43.6	2.22	1.05
	0	−	−	0.46	94.5	1.3	4.0	4.6	1.33	0.57	1.02
	0.6	−	−	0.47	69.2	2.0	25.5	4.9	5.2	1.08	0.98
W333F	0.9	−	−	0.45	22.3	1.6	49.4	3.7	28.3	1.98	0.94
	2	−	−	0.39	19.5	1.3	40.8	3.0	39.7	1.86	0.98
	5	−	−	0.41	20.9	1.4	40.0	3.0	38.6	1.89	1.03

[a] At 20 °C and pH 7.5, with excitation at 300 nm and emission detected above 324 nm. τ_i is the fluorescence lifetime, A_i the relative amplitude, and $\langle\tau\rangle$ the average fluorescence lifetime.

both tryptophans, due to either slightly different absorption coefficients in the red edge (300 nm) or some apparent "static" quenching of the highly quenched tryptophan 333.

Time-Resolved Fluorescence Study of the Denaturation Process Induced by Gdm-Cl. The fluorescence decays of the wild-type yPGK and the two mutants in the presence of 5 M Gdm-Cl show in all cases three lifetimes close to similar values at 0.34, 1.4, and 3.5 ns, with comparable weights, and an average fluorescence lifetime of about 2 ns (Figure 4D−F and Table 5). The similarity of the lifetime distributions observed on the three denatured proteins shows that the specific structural determinants of the fluorescence emission of each tryptophan residue in the native protein are almost lost. The lifetime distributions are broad and strongly heterogeneous, reflecting large conformational fluctuations around the tryptophan residues in these denatured forms. One of the lifetimes (0.4 ns) is similar to a major component observed in the three native forms of yPGK. The longer ones (1.4 and 3.5 ns) also overlap with some long lifetimes observed with minor weights in the native forms. However, they are strongly dominating the emission of the denatured proteins and can thus be used, as suggested by Szpikowska et al. (*23*), as reporters of the denaturation process.

The fluorescence decays of the wild-type yPGK and the two mutants have been studied along the Gdm-Cl-induced denaturation transition, with special interest for the transition midpoints and for the points corresponding to the so-called hyperfluorescent state in each protein (Figure 5 and Table 5).

It has been proposed that, in their hyperfluorescent states, the two tryptophans are surrounded by residual structures and should therefore be located in an environment different from that in the fully denatured state (*20*). The average fluorescence lifetimes determined along the denaturation process are, within error bars, in rough agreement with the observed steady state intensities (*20*). However, the comparison of the fluorescence lifetime distributions obtained at the hyperfluorescent points with the ones obtained for the denatured states at 5 M Gdm-Cl does not show a significant difference. On one hand, the average lifetime and the prin-

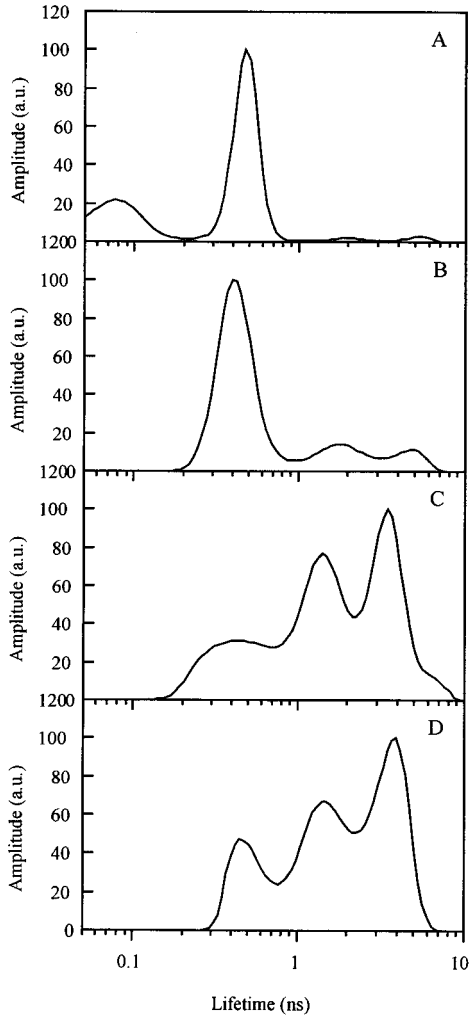

FIGURE 5: Tryptophan fluorescence lifetime distributions of wild-type yPGK with increasing concentrations of Gdm-Cl: (A) 0 M, (B) 0.7 M (midpoint transition), (C) 1 M (hyperfluorescent state), and (D) 5 M Gdm-Cl (fully denatured).

cipal components separated in the distributions are very similar (Table 5). On the other hand, the slight differences in shape between the respective distributions remain within the range of the large experimental dispersions that affect the recovery of such complex profiles (Figure 5).

The presence or absence of these residual structures therefore does not seem to perturb to a large extent the fluorescence kinetics of the tryptophan residues. In fact, a deconvolution of the yPGK steady state fluorescence transition curves according to a three-state process shows that, at the denaturant concentration corresponding to the hyperfluorescent state, the proportion of this particular species does not exceed about 50%. Therefore, its detection under the equilibrium conditions of our measurements would require the accurate demonstration of (possibly small) perturbations within a mixture of species, all of them having very complex fluorescence kinetics. Clearly, these are conditions where the resolving power of time-resolved fluorescence collapses dramatically (*39*).

One important aspect of this new denaturation study by time-resolved fluorescence is that the assignment of some lifetimes to specific tryptophan residues allows us to study the changes in their respective environment directly within the wild-type yPGK. For a Gdm-Cl concentration (0.7 M) corresponding to the transition midpoint in wild-type yPGK, the 0.1 ns lifetime associated with tryptophan 333 in the native protein is lacking in the lifetime distribution (Figure 5), while the amplitudes of the two long components, considered as tracers of denatured yPGK, increase. However, they both remain at a relatively low level, showing that the protein is not yet completely in a denatured state. Meanwhile, the amplitude associated with the 0.5 ns lifetime transiently increases from 69 to 78%, before decreasing to about 20% when going toward the completely denatured state (Table 5). This biphasic behavior may be explained if the corresponding lifetime includes at least two superimposed contributions; indeed, the increase at 0.7 M Gdm-Cl might correspond to the unchanged dominant contribution of tryptophan 308 in its native environment, plus the increased amplitude of a similar lifetime associated with the denatured tryptophan 333. Then, it seems that the changes that modify the conformation of the wild-type yPGK for this Gdm-Cl concentration mainly alter the microenvironment of tryptophan 333, while at the same time, that of tryptophan 308 does not seems to be much perturbed.

DISCUSSION

Major Components in the Fluorescence Emission of Wild-Type and Mutant yPGK. The fluorescence decay of each of the two tryptophan residues in native yPGK is a complex process, both of which are characterized by a multiplicity of lifetimes. As a result, both residues give significant contributions to nearly all fluorescence lifetimes present in the wild-type enzyme. This nicely confirms previous suggestions by Dryden and Pain (*29*), who constructed Stern−Volmer plots from time-resolved acrylamide-quenching studies. The strong nonlinearity of these plots forced the puzzling conclusion that all three lifetimes separated at that time in the fluorescence of wild-type yPGK were actually heterogeneous, all of them including a completely inaccessible fraction. From what we know today of both tryptophan 333 fluorescence (Figure 4) and accessibility to acrylamide (Table 2), it is clear that this inaccessible fraction corresponds precisely to the emission of this residue.

The construction of two single-tryptophan mutants and their careful study permit in addition a more detailed assignment of some lifetime component to each particular emittor. The decay of the wild-type protein is thus principally influenced by two exponential terms. Tryptophan 333 is characterized by a very efficient fluorescence quenching, leading to the shorter fluorescence lifetime of 0.1 ns. Tryptophan 308 also has a quenched fluorescence, although it is less efficiently quenched than that of tryptophan 333, and makes its major contribution to the fluorescence with a nearly single term at 0.5 ns. As has been proposed previously (*28*), aspartate in position 287, located at 4 Å of the indole ring in the native protein, is a good candidate for the quenching of tryptophan 308 fluorescence. On the other hand, the observation of the three-dimensional structure (*21*) does not allow for determination of the exact origin of the very strong fluorescence quenching of tryptophan 333. As no charged residue can be observed in the environment of this tryptophan, it can be assumed that a carbonyl group of the backbone in the vicinity of tryptophan 333 is responsible for this phenomenon.

The lifetime assignment obtained allows in addition a specific monitoring of the conformational state around each of the two tryptophan residues in wild-type yPGK. During Gdm-Cl-induced denaturation, as assessed by time-resolved fluorescence spectroscopy, a prior perturbation of the microenvironment of tryptophan 333 relative to that of tryptophan 308 is observed. These results, together with those of Sherman et al. (*48*), show that the denaturation of yPGK implies successive steps involving different parts of the structure, with half-transitions C_m ranging from 0.5 M for the region around tryptophan 333 to 0.9 M around tryptophan 48 in the N-terminal domain (*48*). This shows clearly that the yPGK denaturation process does not correspond to a two-state model. Nevertheless, it should be kept in mind that the perturbations of tryptophan fluorescence emission may be due to relatively local events, which do not imply that complete domains of the protein are fully and sequentially denatured (see below).

Significance of Minor Long Lifetime Components in Native yPGK. The various native yPGKs studied here also include several long fluorescence lifetimes, which are observed in variable proportions in all samples. It has been suggested before (*23*) that these long components would represent a certain amount of denatured protein present in all preparations. This suggestion was based on the observation of similar long lifetimes in denatured yPGK. However, it is clear that a similarity in fluorescence lifetime is far from being sufficient for the unambiguous identification of the species concerned. It seems therefore interesting to recall, at this point, all we know about these long lifetime species from past and current literature.

First, their relative weight in the kinetics varies strongly depending on the authors. We propose to account for these variations by the variable levels of instrumentation resolution, leading to different efficiencies in the detection of the short yPGK lifetimes, as suggested by the results in Table 4. Privat et al. (*28*) have shown also that the relative weight of these long lifetimes increases strongly in the low pH range, which possibly reflects an acid denaturation of the protein (unpublished observations in our laboratory). Privat et al. (*28*) and Wasylewski and Eftink (*27*) have shown that these long components are associated with a preferential emission in the red ($\lambda_{max} = 338$ nm), while in acrylamide quenching studies, an accessible fraction of the yPGK fluorescence was also shown by Dryden and Pain (*29*) to be associated with a red-shifted emission. In addition, we found that, in W333F and wild-type yPGK, some long fluorescence lifetime components are specifically associated with a high rotational mobility (preliminary unpublished time-resolved fluorescence anisotropy data). In the mutant W308Y, tryptophan 333 exhibits on the average a high rotational mobility, and thus, a possible flexibility associated with its long fluorescence lifetimes could be masked.

Therefore, it is indeed tempting to follow the proposed global assignment of the long lifetimes in yPGK to some type of "denatured" contaminant. However, things may be a bit more complex if one takes into account additional sets of information. First, W308Y is the mutant where these long components are observed with the highest amplitude, contributing to more than 65% of its total fluorescence intensity. However, the emission of this mutant is preferentially blue-shifted, with a maximum around 320−330 nm, while

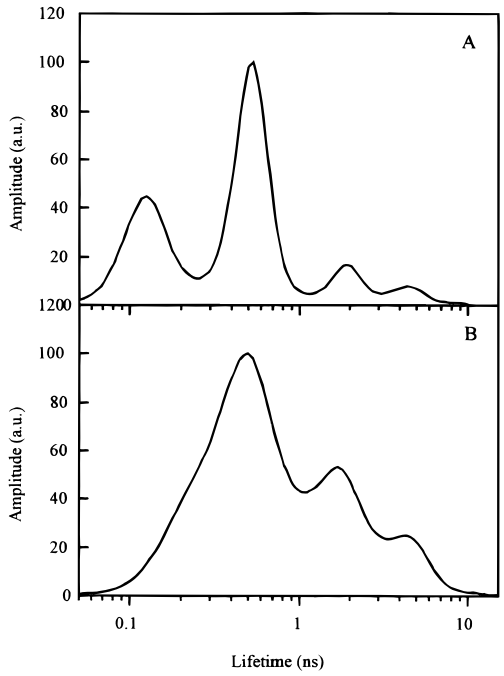

FIGURE 6: Tryptophan fluorescence lifetime distributions of mutant yPGK Δ404−415 in the absence (A) and presence (B) of 0.25 M Gdm-Cl.

Szpikowska et al. (*23*) report similar blue emission for their mutant W308F. Tryptophan 333 in our mutant as well as in the wild-type protein also appears to be completely inaccessible to acrylamide. Therefore, it seems more likely that, in the case of tryptophan 333, the multiple long lifetimes observed reflect multiple conformations of the side chain, arising from a relatively high degree of local mobility (see above). As a consequence, the long lifetimes possibly associated with an exposed and mobile form would be more specifically ascribed to tryptophan 308, which would be in line with the previous assignments of Dryden and Pain (*29*). These forms would represent less than 2−5% of the total population of this residue, but may contribute to 10−20% of its steady state fluorescence intensity, depending on the detection conditions. Complete decay-associated spectra should be constructed, and excitation wavelength studies should be performed, to reach an accurate quantification of this population.

It must be stressed that these long lifetimes are not forcedly associated with some globally denatured state of the protein, but rather with some minor conformation having very different local interactions and dynamics at the level of the tryptophan residue. To illustrate this, we show in Figure 6 the fluorescence lifetime distribution obtained on another, previously described, destabilized mutant, yPGK Δ404−415 (*49*). Although it is strongly inactivated compared to the wild-type enzyme, this mutant was shown previously to retain most of its global secondary structure and activity up to 0.5 M Gdm-Cl. However, well below this point, at 0.25 M Gdm-Cl, the major specific features of the native yPGK fluorescence lifetime distribution are lost, with the appearance of high weights of long lifetime components (Figure 6B). This locally perturbed and yet active state of yPGK Δ404−415 is, in addition, under fully reversible equilibrium with the native form.

Possible Implications for the Steady State Hyperfluorescent State. The biphasic transition observed by following the tryptophan fluorescence intensity during the unfolding process, which is the basis for the so-called hyperfluorescent state (*20*), could be due to the successive denaturation of two species initially coexisting in native samples. The first transition, associated with an increase in fluorescence intensity, would then be due to the prior denaturation of a less stable, "nonflexible" protein (characterized by short fluorescence lifetimes), while the second transition, accompanied by a decrease in fluorescence intensity, would be due to the subsequent unfolding of a more stable but more flexible species (characterized by longer fluorescence lifetimes). However, the reversibility of the process implies that these species are under fully reversible equilibrium (*20*). In this case, there is no simple scheme to account for a thermodynamic equilibrium between a major species and another more stable one, but present in low proportions.

Biphasic transitions passing through a hyperfluorescent intermediate have been observed in yPGK by monitoring the fluorescence of several natural or mutated single tryptophan residues located in very different parts of the yPGK structure. Beside tryptophans 308 and 333, located respectively in the C-terminal domain, similar and even more pronounced hyperfluorescent intermediates have been demonstrated for tryptophans inserted at positions 122 and 458 in the N-terminal domain (*48*). Actually, the observation of such a hyperfluorescent state seems to be roughly correlated with tryptophan residues having a relatively low quantum yield in the native state of yPGK. It may be due to the fact that similar biphasic transitions simply escape detection in other cases (such as genetically engineered tryptophans 194 and 399) because, for tryptophan with high initial fluorescence intensities, the two successive transitions are both accompanied by a decrease in fluorescence signal and thus cannot be distinguished. While the observation of hyperfluorescent states in the denaturation process of yPGK seems to be a rather frequent phenomenon, our study of the residual structures suggests that these states may result from rather different molecular interactions.

Nature of the Residual Structures in Wild-Type and Mutant yPGK. It is now generally admitted that residual structures are important for the early stages of the folding process. The existence of such short-range interactions in an unfolded polypeptide chain could "guide" the protein matrix toward an intermediate conformation, therefore reducing the search of a three-dimensional structure through conformational space and acting as an initiation center of the folding process (*15*, *50)*.

The results presented in this paper have produced a more detailed characterization of the residual structures existing in the hyperfluorescent state of yPGK. The denaturation curves obtained at low temperatures suggest that the residual structures corresponding to the tryptophan 308 environment are mainly stabilized by hydrophobic interactions. During fluorescence quenching studies by acrylamide, the comparison of the static and collisional quenching constants indicates that both tryptophans are involved in residual structures in the hyperfluorescent intermediate, although tryptophan 333 seems to be involved in less compact and more dynamic microstructures.

A few hydrophobic residues are close to tryptophan 308 in the sequence. It thus seems likely that this tryptophan is interacting with isoleucine 304, alanine 306, and/or leucine 311 in these residual structures. The hydrophobic collapse, the structure of which was determined by Neri et al. (*3*), is also stabilized by interactions between a tryptophan residue and aliphatic chains. In the α-subunit of tryptophan synthase (*11*, *12*), monodimensional NMR has shown that histidine 92 in this protein was involved in residual structures in the presence of 5 M urea. Similarly, the absence of these microstructures with 5 M urea at low temperatures and the hydrophobic environment of histidine 92 in the sequence had suggested a hydrophobic origin for the stabilization of these structures. The mutation of hydrophobic residues close to tryptophan 308 in the yPGK structure would allow us to point out the residues involved in these interactions. On the other hand, the microstructures around tryptophan 333 could be related to the persistence of native secondary structures as found in the denatured states of various proteins (*8*, *9*, *51)*.

A further step in the characterization of residual structures in the denatured state of yPGK would include a NMR analysis. However, the dispersion of nuclear resonance decreases when a protein-folded state breaks down, leading to a particularly severe overlap of peaks for a protein as large as yPGK. A different approach would be the synthesis of small peptides including the residues surrounding the tryptophans in the sequence and their study by heteronuclear NMR. As the interactions stabilizing these residual structures are supposed to be short-range ones, they should persist in small peptides. A more detailed picture of these collapses could therefore be afforded.

ACKNOWLEDGMENT

We thank the LURE technical staff for running the synchrotron machine and the computing facilities.

REFERENCES

1. Evans, P. A., Topping, K. D., Woolfson, D. N., and Dobson, C. M. (1991) *Proteins: Struct., Funct., Genet. 9*, 248−266.
2. Neri, D., Wider, G., and Wüthrich, K. (1992) *Proc. Natl. Acad. Sci. U.S.A. 89*, 4397−4401.
3. Neri, D., Billeter, M., Wider, G., and Wüthrich, K. (1992) *Science 257*, 1559−1563.
4. Sosnick, T. R., and Trewella, J. (1992) *Biochemistry 31*, 8329−8335.
5. Buckler, D. R., Haas, E., and Scheraga, H. A. (1995) *Biochemistry 34*, 15965−15978.
6. Gottfried, D. S., and Haas, E. (1992) *Biochemistry 31*, 12353−12362.
7. Lumb, K. J., and Kim, P. S. (1994) *J. Mol. Biol. 236*, 412−420.
8. Logan, T. M., Thériault, Y., and Fesik, S. W. (1994) *J. Mol. Biol. 236*, 637−648.
9. Arcus, V. L., Vuilleumier, S., Freund, S. M. V., Bycroft, M., and Fersht, A. R. (1995) *J. Mol. Biol. 254*, 305−321.
10. Wong, K. B., Freund, S. M. V., and Fersht, A. R. (1996) *J. Mol. Biol. 259*, 805−818.
11. Saab-Rincón, G., Frœbe, C. L., and Matthews, C. R. (1993) *Biochemistry 32*, 13981−13990.
12. Saab-Rincón, G., Gualfette, P. J., and Matthews, C. R. (1996) *Biochemistry 35*, 1988−1994.
13. Dobson, C. M. (1992) *Curr. Opin. Struct. Biol. 2*, 6−12.
14. Shortle, D. (1993) *Curr. Opin. Struct. Biol. 3*, 66−74.
15. Shortle, D. (1996) *Curr. Opin. Struct. Biol. 6*, 24−30.
16. Miranker, A. D., and Dobson, C. M. (1996) *Curr. Opin. Struct. Biol. 6*, 31−42.

17. Garvey, E. P., and Matthews, C. R. (1989) *Biochemistry 28*, 2083−2093.
18. Garvey, E. P., Swank, J., and Matthews, C. R. (1989) *Proteins: Struct., Funct., Genet. 6*, 259−266.
19. James, E., Wu, P. G., Stites, W., and Brand, L. (1992) *Biochemistry 31*, 10217−10225.
20. Garcia, P., Desmadril, M., Minard, P., and Yon, J. M. (1995) *Biochemistry 34*, 397−404.
21. Watson, H. C., Walker, N. P. C., Shaw, P. J., Bryant, T. N., Wendell, P. L., Fothergill, L. A., Perkins, R. E., Conroy, S. C., Dobson, M. J., Tuite, M. F., Kingsman, A. J., and Kingsman, S. M. (1982) *EMBO J. 1*, 1635−1640.
22. Missiakas, D., Betton, J. M., Minard, P., and Yon, J. M. (1990) *Biochemistry 29*, 8683−8689.
23. Szpikowska, B. K., Beechem, J. M., Sherman, M. A., and Mas, M. T. (1994) *Biochemistry 33*, 2217−2225.
24. Baldwin, R. L. (1986) *Proc. Natl. Acad. Sci. U.S.A. 83*, 8069−8072.
25. Dill, K. A., Darwin, O., Alonso, V., and Hutchinson, K. (1989) *Biochemistry 28*, 5439−5449.
26. Dill, K. A. (1990) *Biochemistry 29*, 7133−7155.
27. Wasylewski, Z., and Eftink, M. R. (1987) *Eur. J. Biochem. 167*, 513−518.
28. Privat, J. P., Wahl, P., and Auchet, J. C. (1980) *Biophys. Chem. 11*, 239−248.
29. Dryden, T. F., and Pain, R. H. (1989) *Biochim. Biophys. Acta 997*, 313−321.
30. Stark, G. R. (1965) *Biochemistry 4*, 1030−1036.
31. Nozaki, Y. (1970) *Methods Enzymol. 26*, 43−50.
32. Warren, J. R., and Gordon, J. A. (1970) *J. Biol. Chem. 245*, 4097−4104.
33. Press, W. H., Flannery, B. P., Tenkolsky, S. A., and Vetterling, W. T. (1986) in *Numerical Recipes*, Cambridge University Press, Cambridge, U.K.
34. Eftink, M. R., and Hagaman, K. A. (1986) *Biophys. Chem. 25*, 277−282.
35. Parker, C. A. (1968) *Photoluminescence of solutions*, pp 220−222, Elsevier, New York.
36. Eftink, M. R., and Ghiron, C. A. (1981) *Anal. Biochem. 114*, 199−227.
37. O'Connor, D. V., and Phillips, D. (1984) in *Time-correlated single photon counting*, Academic Press, London.
38. Blandin, P., Mérola, F., Brochon, J. C., Trémeau, O., and Ménez, A. (1994) *Biochemistry 33*, 2610−2619.
39. Mérola, F., Blandin, P., Brochon, J. C., Trémeau, O., and Ménez, A. (1995) *J. Fluoresc. 5*, 205−215.
40. Livesey, A. K., and Brochon, J. C. (1987) *Biophys. J. 52*, 693−706.
41. Eftink, M. R. (1991) in *Topics in Fluorescence Spectroscopy* (Lakowicz, J. R., Ed.) Vol. 2, pp 53−127, Plenum Press, New York.
42. Smith, C. J., Clarke, A. R., Chia, W. N., Irons, L. I., Atkinson, T., and Holbrook, J. J. (1991) *Biochemistry 30*, 1028−1036.
43. Eftink, M. R., and Ghiron, C. A. (1976) *J. Phys. Chem. 80*, 486−493.
44. Eftink, M. R., and Ghiron, C. A. (1976) *Biochemistry 15*, 672−680.
45. Minard, P., Desmadril, M., Ballery, N., Perahia, D., Mouawad, L., Hall, L., and Yon, J. M. (1989) *Eur. J. Biochem. 185*, 419−423.
46. James, D. R., and Ware, W. R. (1985) *Chem. Phys. Lett. 120*, 455−459.
47. Alcala, J. R., Gratton, E., and Prendergast, F. G. (1987) *Biophys. J. 51*, 587−596.
48. Sherman, M. A., Beechem, J. M., and Mas, M. T. (1995) *Biochemistry 34*, 13934−13942.
49. Ritco-Vonsovici, M., Mouratou, B., Minard, P., Desmadril, M., Yon, J. M., Andrieux, M., Leroy, E., and Guittet, E. (1995) *Biochemistry 34*, 833−841.
50. Wüthrich, K. (1994) *Curr. Opin. Struct. Biol. 4*, 93−99.
51. Shortle, D., and Abeygunawardana, C. (1973) *Structure 1*, 121−134.

BI973161X